UDC 539.12.04:621.793:548.73

STRUCTURE AND CORROSION RESISTANCE OF VACUUM-ARC MULTI-PERIOD CrN/Cu, ZrN/Cu, AND NbN/Cu COATINGS

H.O. Postelnyk[1], O.V. Sobol'[1], V.A. Stolbovoy[2], I.V. Serdiuk[2], O. Chocholaty[3]
[1]National Technical University "Kharkiv Polytechnic Institute", Kharkiv, Ukraine
E-mail: sool@kpi.kharkov.ua;
[2]National Science Center "Kharkov Institute of Physics and Technology", Kharkiv, Ukraine;
[3]University of West Bohemia, Pilsen, Czech Republic
E-mail: chochola@kmm.zcu.cz

The structure and properties of vacuum-arc multi-period composite coatings of the MeN/Cu system (where Me is Cr, Zr, and Nb) are studied. It was found that at the smallest nanolayer thickness (about 8…10 nm) of composites in the layers of all systems, only a phase with an fcc lattice is formed, without a pronounced texture in the nitride layers. For ZrN and CrN, the phases with an fcc lattice are equilibrium, and for NbN, they are nonequilibrium. An increase in the thickness of nitride layers leads to the appearance of a texture in ZrN/Cu and CrN/Cu systems and the formation of an equilibrium ε-NbN phase in the layers of the NbN/Cu system. Tests for corrosion resistance in the environment of the formation of chloride ions showed that the coatings are anodic reaction. The best corrosion properties were obtained for coatings with the smallest layer thickness (about 8…10 nm).

INTRODUCTION

Of great practical interest is the study of the corrosion properties of materials, because this is the basis for their use in biomedical engineering, the electrical industry, power engineering and other fields. Traditional methods for increasing corrosion resistance are the deposition of corrosion-resistant coatings on the surface of products [1–4], the use of corrosion inhibitors [5], etc. Among these methods, the most universal method is the production of protective coatings based on nanocomposites [6, 7]. Such coatings provide an increase in the whole complex of physicomechanical surface characteristics [8]. It should be noted that the deposition process from ion-plasma flows of coatings occurs under highly nonequilibrium conditions [9, 10]. Under these conditions, structural engineering [11] is the most effective way of directional changing the structure and properties. As a result of using this method, it was possible to create vacuum-arc multi-period coatings based on transition metal nitrides with very high physical and mechanical properties [12]. In such nanocomposites, the use of CrN layers is associated with their high wear resistance and oxidation resistance [13, 14]; the use of ZrN is associated with high erosion resistance, strength in combination with high hardness, ZrN is also a radiation-resistant material [15], and NbN is with high hardness, wear resistance, and oxidation resistance [16, 17]. All of these nitride coatings are corrosion resistant and work well in aggressive environments.

Adding a second "immiscible" transition metal (for example, copper) makes it possible to increase the plastic properties of the coatings and reduces the likelihood of brittle chip, which is especially important for biomedical applications.

The aim of this work was to study the influence of technological conditions for the preparation of different-type multi-period composites based on nitrides of transition metals and copper on their phase-structural state and electrochemical characteristics of corrosion in physiological saline using mutually complementary methods: open-circuit potential, impedance spectroscopy, and potentiodynamic polarization.

SAMPLES AND RESEARCH METHODS

The coatings were deposited by the vacuum-arc method at the "Bulat-6" installation. Substrates for coating were samples of size 20x20x2 mm made of austenitic stainless steel AISI 321.

Table 1 shows the main technological parameters of the deposition of the studied coatings.

Table 1

Technological parameters of coating deposition

	Series	P_N, Torr	U_b, V	Substrate holder operation mode
CrN/Cu	1	$5\cdot10^{-4}$	-200	constant rotation
	2	$4\cdot10^{-3}$	-65	
	3	$4\cdot10^{-3}$	-65	20 s interval 180 layers
ZrN/Cu	4	$3\cdot10^{-3}$	-110	constant rotation
	5	$3\cdot10^{-3}$	-70	
	6	$3\cdot10^{-3}$	-200	
NbN/Cu	7	$7\cdot10^{-4}$	-50	
	8	$3\cdot10^{-3}$	-50	
	9	$7\cdot10^{-4}$	-50	20 s interval 180 layers
	10	$7\cdot10^{-4}$	-200	
	11	$3\cdot10^{-3}$	-100	120 s – Cu 300 s – Nb

The pressure of the working atmosphere (P_N) ranged from $4\cdot10^{-3}$ to $5\cdot10^{-4}$ Torr; the bias potential supplied to the substrate varied from -50 to -200 V. The deposition was carried out from two sources. The first source is Cr, Zr or Nb, depending on the type of coating, the second source is Cu; in a mode with a constant rotation speed (rotation speed of 8 rpm) and in discrete mode (with a stop for 20 s near each of the plasma sources of series 1 (CrN/Cu), 9 and 10 (NbN/Cu), as well as with a stop 120 and 300 s for Cu and Nb layers (series 11),

respectively, with a total coating time of 1.5 h and a coating thickness of about 12 μm.

The phase-structural state was studied by X-ray diffractometry using a DRON-4 apparatus in Cu-Kα radiation using θ-2θ scanning with a monochromator on a secondary beam [18]. To decode the diffraction patterns, tables of the international Powder Diffraction File center were used [19].

The coatings were examined for their corrosion resistance during electrochemical processes. Electrochemical tests were carried out using a 3-electrode cell with a volume of 200 ml and a Biologic SP-150 potentiostat. The cell consists of a coated sample (working electrode), a saturated calomel electrode (reference electrode), and a platinum electrode (counter electrode). Corrosion resistance was evaluated by measuring the open-circuit potential for 1.5 h in a solution of 0.9% NaCl at room temperature.

Impedance spectroscopy was performed in the frequency range from 10^{-2} to 10^{5} Hz. The potentiodynamic polarization test was carried out in the range from -0.6 to +1 V at a scanning speed of 1 mV/s. The contact area of the sample with the electrolyte was 0.196 cm^2.

RESULTS AND DISCUSSION

To study the phase-structural state, the XRD method was used. X-ray diffraction spectra of all studied coatings are shown in Figs. 1–3.

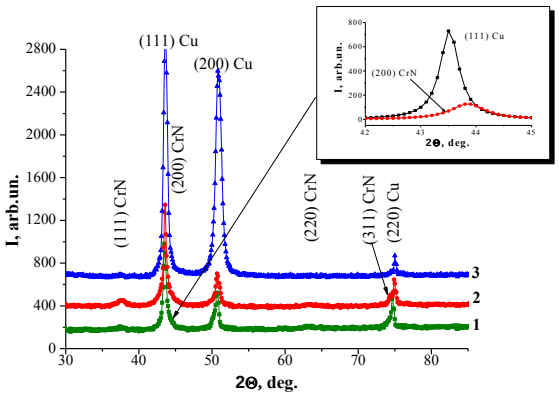

Fig. 1. Plots of the diffraction spectra of CrN/Cu coatings and decomposition of the complex diffraction profile of series 1 into components (insert in the upper right corner): 1 – P_N = 5·10^{-4} Torr, U_b = -200 V (continuous operation); 2 – P_N = 4·10^{-3} Torr, U_b = -65 V (continuous mode); 3 – P_N = 4·10^{-3} Torr, U_b = -65 V (discrete mode, 20 s)

From the spectra in Fig. 1 (CrN/Cu nanocomposite) it can be seen that the positions of the diffraction peaks correspond to the fcc lattices of the two phases CrN (JCPDS 76-2494) and Cu (JCPDS 89-2838). The relatively high intensity of the (111) CrN peak for series 2 samples (see spectrum 2, Fig. 1) indicates the presence in the CrN layers of a predominant orientation of crystallites with the [111] axis perpendicular to the growth plane. The lattice periods calculated from the position of the peaks remain practically unchanged for the Cu layers and amount to a_{Cu} = 0.3595 nm. Changes in the lattice period are observed for CrN layers. The smallest value is a_{CrN} = 0.4140 nm (for samples of series 2), and for samples of series 1 and 3, the period is somewhat longer and is a_{CrN} = 0.4157 (1 series) and a_{CrN} = 0.4154 nm (3 series). The most likely cause of this change is the formation of a stress-strain state of compression in CrN layers.

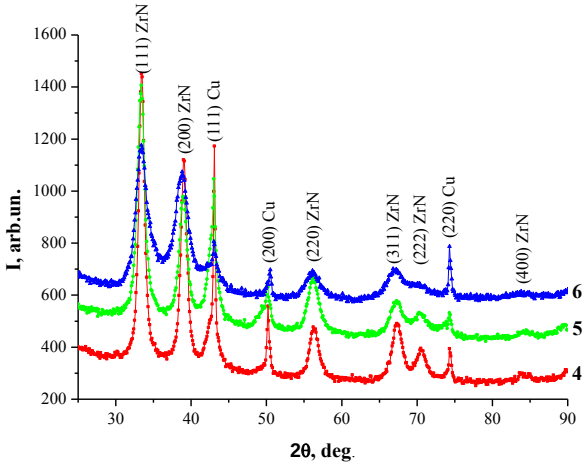

Fig. 2. Plots of diffraction spectra of ZrN/Cu multilayer coatings under continuous deposition: 4 – P_N = 3·10^{-3} Torr, U_b = -110 B; 5 – P_N = 3·10^{-3} Torr, U_b = -70 V; 6 – P_N = 3·10^{-3} Torr, U_b = -200 V

Fig. 2 shows that for the multi-period ZrN/Cu nanocomposite, diffraction peaks inherent in the 2 phases are also revealed: ZrN (JCPDS 78-1420) and Cu, with a face-centered cubic lattice (structural type NaCl). The lattice period for copper layers remains practically unchanged for different deposition modes and amounts to a_{Cu} = 0.3611 nm. In ZrN layers, a change in the lattice period is observed. So, for samples of series 4 – a_{ZrN} = 0.4629 nm, series 5 – a_{ZrN} = 0.4632 nm, series 6 – a_{ZrN} = 0.4635 nm. Such a change in the lattice period is also apparently related to the action of compression stresses in ZrN layers.

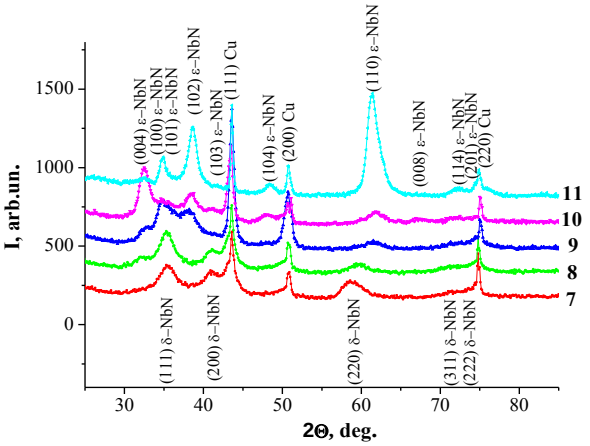

Fig. 3. Plots of diffraction spectra of NbN/Cu multilayer coatings: 7 – P_N = 7·10^{-4} Torr, U_b = -50 V (continuous operation); 8 – P_N = 3·10^{-3} Torr, U_b = -50 V (continuous operation); 9 – P_N = 7·10^{-4} Torr, U_b = -50 V (discrete mode, 20 s); 10 – P_N = 7·10^{-4} Torr, U_b = -200 V (discrete mode, 20 s); 11 – P_N = 3·10^{-3} Torr, U_b = -100 V (discrete mode, 120 s for Cu layers and 300 s for NbN)

For the NbN/Cu nanocomposite, it is seen that at a relatively low pressure $P_N = 7 \cdot 10^{-4}$ Torr (see spectrum 7, Fig. 3), in the constant rotation mode, two phases form with an fcc crystal lattice: metastable δ-NbN (JCPDS 38-1155) and Cu. The ratio of peak intensities is close to the standard for the fcc lattice, which indicates the absence of a pronounced texture. The lattice period for copper is a_{Cu} = 0.3590 nm, and for $a_{\delta\text{-NbN}}$ = 0.4455 nm (samples of series 7) and $a_{\delta\text{-NbN}}$ = 0.4368 nm (samples of series 8). An increase in pressure to $3 \cdot 10^{-3}$ Torr (see spectrum 8, Fig. 3) leads to a qualitative change in diffraction spectra. Changes are also associated with the appearance of diffraction peaks from the equilibrium ε-NbN (JCPDS 89-4757) phase with a hexagonal crystal lattice.

An increase in the layer thickness to 40 nm (20 s interval, spectra 9, 10, see Fig. 3) leads to the formation of only the equilibrium ε-NbN phase and Cu. An increase in the bias potential to U_b = -200 V (see spectrum 10, Fig. 3) does not lead to a change in the phase composition. However, in this case, the preferred orientation of crystallites with the (004) plane perpendicular to the growth surface is formed.

With the greatest thickness, a complete spectrum of diffraction peaks of ε-NbN and Cu phases is formed without a noticeable preferential orientation (see spectrum 11, Fig. 3).

The lattice period for ε-NbN is: $a_{\varepsilon\text{-NbN}}$ = 0.3016 nm (series 9), $a_{\varepsilon\text{-NbN}}$ = 0.3003 nm (series 10), $a_{\varepsilon\text{-NbN}}$ = = 0.3020 nm (series 11).

Thus, a comparison of the phase-structural states for multi-period CrN/Cu, ZrN/Cu, and NbN/Cu nanocomposites shows that the formation of a two-phase state with an fcc crystal lattice is typical for all types of coatings except NbN/Cu (samples of series 8–11). The lattice period calculated from the position of the diffraction peaks for copper layers remains almost unchanged for all types of coatings, while for the CrN, ZrN, and NbN layers it changes. A shift towards lower diffraction angles with the θ-2θ survey scheme indicates the formation of a stress-strain state of compression in these layers.

Electrochemical tests of the coatings were carried out using a 3-electrode cell with a volume of 200 ml.

Fig. 4 shows plots of corrosion potential versus time.

As can be seen from the curves in Fig. 4,a, a series 3 coating (CrN/Cu nanocomposite) obtained in the discrete mode (with an interval of 20 s) is characterized by a sharp dissolution of the coating (the first minute of testing) followed by passivation. Sharp peaks and changes in the nature of the curve can indicate damage to the passivating layer and the protective coating as a whole.

Samples of CrN/Cu coatings obtained in other modes (see series 1, 2, Fig. 4,a) tend to passivate and soperpassivate, which is associated with an increase in the valence of chromium (Cr^{3+}) with the implementation of reactions:

$$Cr(OH)_3 + 5OH^- - 3e \rightarrow CrO_4^{2-} + 4H_2O;$$
$$2Cr^{3+} + 7H_2O - 6e \rightarrow Cr_2O_7^{2-} + 14H^+.$$

A series of ZrN/Cu coatings is characterized by weak passivation (see Fig. 4,b). This is due to violation of the continuity of the coating due to brittle fracture and the appearance of copper on the surface, as well as strong internal stresses.

NbN/Cu coatings are characterized by a uniformly slow passivation process (see Fig. 4,c). However, the peaks in the curves of Fig. 4,c indicate the processes of local destruction of coatings (similar to the sample of series 3 (CrN/Cu)).

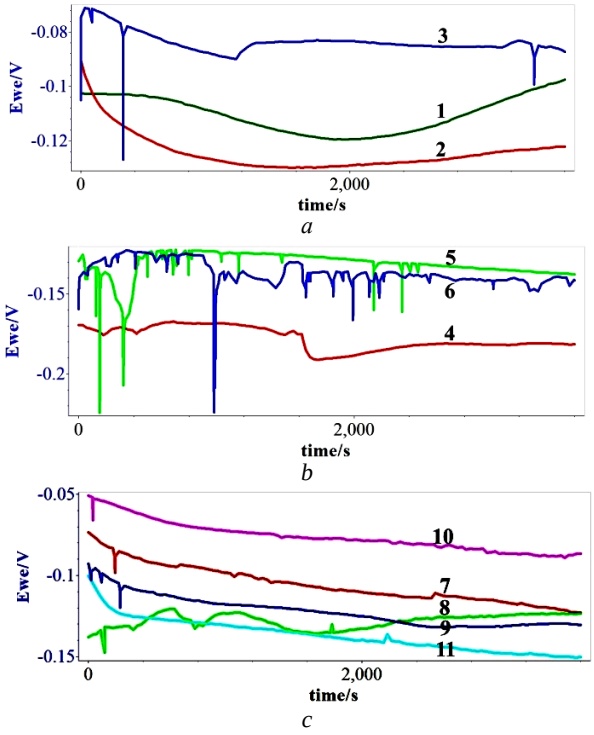

Fig. 4. Plots of corrosion potential versus time: a – CrN/Cu; b – ZrN/Cu; c – NbN/Cu

Fig. 5 shows the potentiodynamic polarization curves of the coatings in physiological saline.

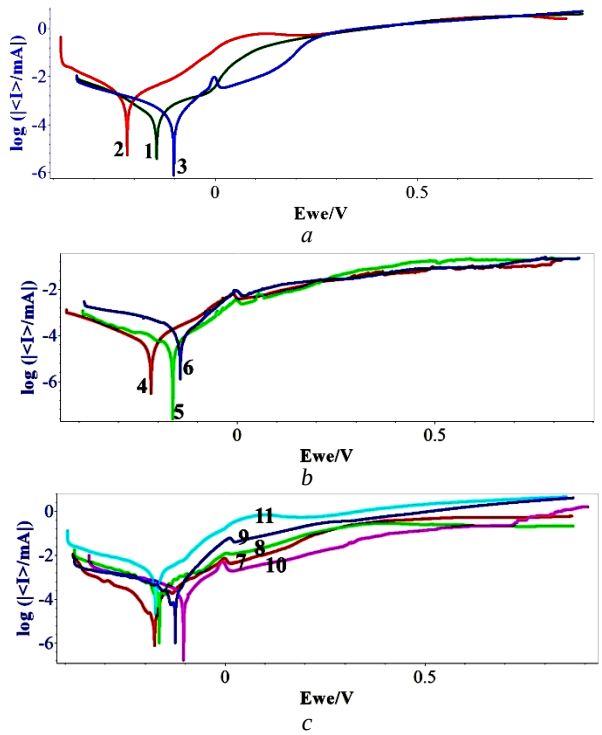

Fig. 5. Potentiodynamic polarization curves: a – CrN/Cu; b – ZrN/Cu; c – NbN/Cu

As can be seen from Fig. 5 – for all coatings, the process is controlled mainly by the anode part of the polarization curves [20].

According to the Tafel extrapolation method, the values of the corrosion potential (E_{corr}), corrosion current density (I_{corr}), anode (β_a) and cathodic (β_c) Tafel tilt can be obtained from polarization curves. The results are shown in Table 2.

Table 2

Corrosion resistance test results

	Series	E_{corr}, mV	I_{corr}, μA	β_a, mV	β_c, mV	CR, mm/year	Rp, Ω·cm^2
CrN/Cu	1	-99.241	0.208	68.3	149.8	$12\cdot10^{-3}$	19208
	2	-200.829	0.872	95.1	106.1	$51.6\cdot10^{-3}$	4900
	3	-229.129	1.692	550.4	218.3	$100\cdot10^{-3}$	7840
ZrN/Cu	4	-206.38	0.044	89.5	159	$2.6\cdot10^{-3}$	110936
	5	-186.861	0.059	118.2	189.2	$3.5\cdot10^{-3}$	105056
	6	-173.411	0.435	163.5	329.9	$26\cdot10^{-3}$	21560
NbN/Cu	7	-208.347	0.09	119.2	103.6	$5.3\cdot10^{-3}$	5252.8
	8	-138.302	0.421	104.2	187.5	$25\cdot10^{-3}$	13563.2
	9	-258.219	1.176	181.7	290	$69\cdot10^{-3}$	8094.8
	10	-303.715	1.96	2155.7	286.3	$116\cdot10^{-3}$	10976
	11	-156.095	2.068	79.4	210.1	$122\cdot10^{-3}$	2352

The corrosion rate is proportional to the corrosion current and was calculated by the formula

$$CR=\frac{I_{corr}\cdot K\cdot EW}{d\cdot A}, \quad (1)$$

where CR is the corrosion rate, mm/year; I_{corr} – corrosion current, mA; K is the conversion factor determining the unit of measurement of the corrosion rate; EW – equivalent weight, gram-equivalent; d is the density, g/cm^3; A is the sample area, cm^2.

To determine the parameter R_p (polarization resistance), the calculation was performed according to the formula

$$R_p=\beta_a\cdot\beta_c/2.303\cdot I_{corr}\cdot(\beta_a+\beta_c) \quad (2)$$

the results of which are given in Table 2.

Samples with a minimum corrosion current have the lowest corrosion rate. The best indicators of the corrosion rate correspond to the regime with a constant speed of rotation (with the smallest layer thickness). So, the most corrosion-resistant are coatings with layers: ZrN – series 4, NbN – series 7, and CrN – series 1.

The charge transfer resistance was also evaluated through protective coatings using Nyquist curves (Fig. 6).

The obtained curves were constructed in accordance with the model of the equivalent electrolyte-coating scheme (Fig. 7).

By comparing the diameters of the loops on the Nyquist graph, we can evaluate the corrosion resistance of the samples: loops of larger diameter correspond to greater corrosion resistance. As can be seen from the Table 2, the corrosion indicators obtained from the calculation of the Tafel curves, and the impedance spectroscopy data have similar trends and confirm the previous conclusions.

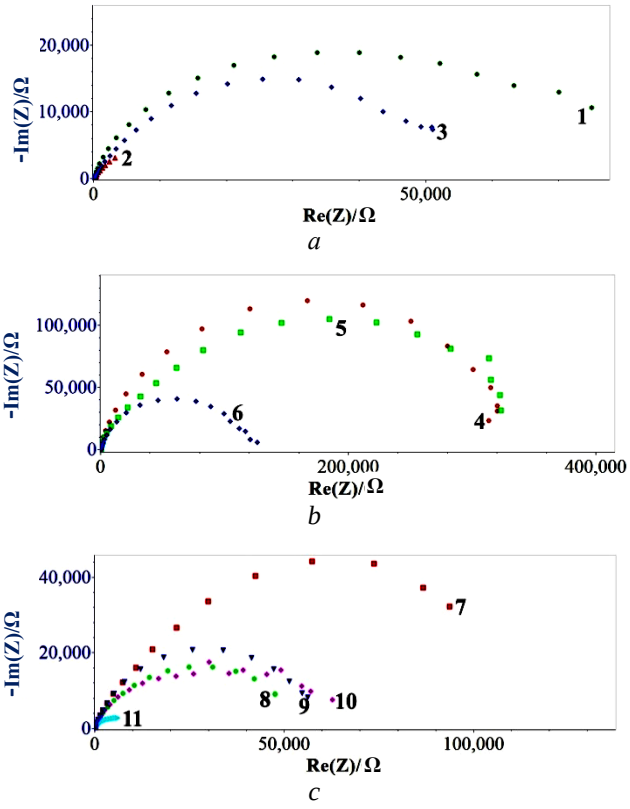

Fig. 6. Nyquist curves: a – CrN/Cu; b – ZrN/Cu; c – NbN/Cu

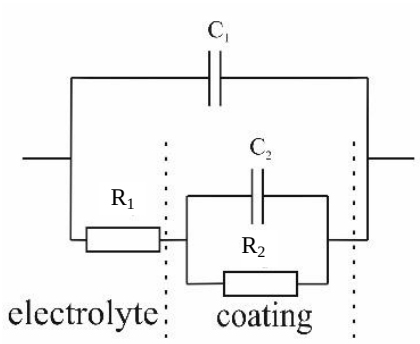

Fig. 7. Model of the equivalent circuit "electrolyte-coating": C_1, C_2 – the capacity of the double layer and coating, respectively; R_1, R_2 – resistance of the electrolyte and phases in the coating, respectively

Based on the results obtained, an assessment was made of the thickness of the protective layers for protection during the year. It was determined that for the annual cycle of coatings in the medium of chloride ion formation, their thickness should correspond to 12 μm for the CrN/Cu system, 2.6 μm to ZrN/Cu, and 5.3 μm to NbN/Cu. Although the CrN/Cu system is inferior in corrosion resistance to the other systems under consideration, the manufacturability of applying in mass practical use as composite coatings should be taken into account.

CONCLUSIONS

Studies of the structure and properties of vacuum-arc coatings showed that only phases with an fcc crystal lattice are formed in the nanolayers of the MeN/Cu composite (Me – Zr, Cr, or Nb), without a pronounced

texture in the nitride layers. For ZrN and CrN, the phases with an fcc lattice are equilibrium, and for NbN, they are nonequilibrium. An increase in the thickness of nitride layers leads to the appearance of a texture in ZrN/Cu and CrN/Cu systems and the formation of an equilibrium ε-NbN phase in the layers of the NbN/Cu system.

Coatings of chromium, zirconium, niobium nitrides with copper nanolayers in the environment of formation of chloride ions, from the point of view of the protective mechanism, are anodic.

The best indicators of corrosion resistance were shown by coatings with the smallest layer thickness of about 8...10 nm, obtained in the constant rotation mode with the following technological parameters: ZrN/Cu ($P_N = 3 \cdot 10^{-3}$ Torr, U_b = -110 V), NbN/Cu ($P_N = 7 \cdot 10^{-4}$ Torr, U_b = -50 V), and CrN/Cu ($P_N = 5 \cdot 10^{-4}$ Torr, U_b = -200 V).

REFERENCES

1. C.L. He, J.L. Zhang, J.M. Wang, G.F. Ma, D.L. Zhao, Q.K. Cai. Effect of strucural defects on corrosion initiation of TiN nanocrystalline films // *Appl. Surf. Sci*. 2013, v. 276, p. 667-671.

2. Q.Z. Wang, F. Zhou, C.D. Wang, M.F. Yuen, M.L. Wang, T. Qian, M. Matsumoto, J.W. Yan. Comparison of tribological and electrochemical properties of TiN, CrN, TiAlN and a-C:H coatings in simulated body fluid // *Mater. Chem. Phys*. 2015, v. 158, p. 74-81.

3. N. Madaoui, B. Zaid, D. Saidi, A.S. Ahmed. Structural, mechanical and electrochemical comparison of TiN and TiCN coatings on XC48 steel substrates in NaCl 3.5% water solution // *Appl. Surf. Sci.* 2014, v. 312, p. 134-138.

4. O.V. Sobol', A.A. Postelnyk, A.A. Meylekhov, A.A. Andreev, V.A. Stolbovoy, V.F. Gorban. Structural Engineering of the multilayer vacuum arc nitride coatings based on Ti, Cr, Mo, and Zr // *Journal of nano- and electronik physics*. 2017, v. 9, issue 3, p. 03003-1–03003-6.

5. A. Aït Aghzzaf, B. Rhouta, E. Rocca, A. Khalil, J. Steinmetz. Corrosion inhibition of zinc by calcium exchanged beidellite clay mineral: a new smart corrosion inhibitor // *Corros. Sci*. 2014, v. 80, p. 46-52.

6. G.T. Parthiban, T. Parthiban, R. Ravi, V. Saraswathy, N. Palaniswamy, V. Sivan. Cathodic protection of steel in concrete using magnesium alloy anode // *Corros. Sci.* 2008, v. 50, p. 3329-3335.

7. O.V. Sobol', A.A. Meilekhov. Conditions of attaining a superhard state at a critical thickness of nanolayers in multiperiodic vacuum-arc plasma deposited nitride coatings // *Technical Physics Letters*. 2018, v. 44(1), p. 63-66.

8. M. Dinu, S.M. Mouele, A.C. Parau, A. Vladescu, L.F. Petrik, and M. Braic. Enhancement of the corrosion resistance of 304 stainless steel by Cr–N and Cr(N,O) coatings // *Coatings.* 2018, v. 8, N 132, p. 1-20.

9. P.H. Mayrhofer, C. Mitterer, L. Hultman, H. Clemens. Microstructural design of hard coatings // *Progress in Materials Science*. 2006, v. 51, p. 1032-1114.

10. O.V. Sobol'. Control of the structure and stress state of thin films and coatings in the process of their preparation by ion-plasma methods // *Physics of the Solid State*. 2011, v. 53(7), p. 1464-1473.

11. O.V. Sobol, A.A. Andreev, V.F. Gorban, A.A. Meylekhov, H.O. Postelnyk, V.A. Stolbovoy. Structural engineering of the vacuum arc ZrN/CrN multilayer coatings // *Journal of nano- and electronic physics*. 2016, v. 8, issue 1, p. 01042-1–01042-4.

12. И.И. Аксенов, Д.С. Аксенов, А.А. Андреев, В.А. Белоус, О.В. Соболь. *Вакуумно-дуговые покрытия. Технология, материалы, структура, свойства*. Харьков: ННЦ ХФТИ, 2015, 379 с.

13. O.V. Sobol, A.A. Andreev, V.F. Gorban. Structure engineering of vacuum-arc multiperiod coatings // *Metal Science and Heat Treatment.* 2016, v. 58 (1), p. 40-42.

14. M. Benkahoul, P. Robin, L. Martinu, J.E. Klemberg-Sapieha. Tribological properties of duplex Cr–Si–N coatings on SS410 steel // *Surf. Coat. Technol*. 2009, v. 203, p. 934-940.

15. O.V. Sobol', A.A. Andreev, V.F. Gorban', V.A. Stolbovoy, A.A. Meylekhov, A.A. Postelnyk. Possibilities of structural engineering in multilayer vacuum-arc ZrN/CrN coatings by varying the nanolayer thickness and application of a bias potential // *Technical Physics*. 2016, v. 61 (7), p. 1060-1063.

16. P. Guzmana, J.L. Caballeroa, G. Orozco Hernándezb, W. Aperadora, J.C. Caicedoc. Tribocorrosion behavior of niobium-based thin films for biomedical applications // *Tribology in Industry.* 2018, v. 40, issue 4, p. 624-632.

17. P. Ren, M. Wen, S.X. Du, Q.N. Meng, K. Zhang, W.T. Zheng. Microstructure, mechanical and tribological properties of NbN/Ni coatings // *Materials Science Forum*. 2017, v. 898, p. 1424-1430.

18. O.V. Sobol', O.A. Shovkoplyas. On advantages of X-ray schemes with orthogonal diffraction vectors for studying the structural state of ion-plasma coatings // *Technical Physics Letters*. 2013, v. 39, issue 6, p. 536-539.

19. http://www.icdd.com

20. C. Ramoul, N.E. Beliardouh, R. Bahi, C. Nouveau, D. Abdelghani, A. Walock. Surface performances of PVD ZrN coatings in biological environments // *Tribology – Materials, Surfaces & Interfaces.* 2018, v. 13, p. 12-19.

Article received 26.12.2019

СТРУКТУРА И КОРРОЗИОННАЯ СТОЙКОСТЬ ВАКУУМНО-ДУГОВЫХ МНОГОПЕРИОДНЫХ CrN/Cu-, ZrN/Cu- И NbN/Cu-ПОКРЫТИЙ

А.А. Постельник, О.В. Соболь, В.А. Столбовой, И.В. Сердюк, O. Chocholaty

Проведено исследование структуры и свойств вакуумно-дуговых многопериодных композиционных покрытий системы MeN/Cu (где Me – Cr, Zr и Nb). Установлено, что при наименьшей толщине нанослоев (около 8…10 нм) композитов в слоях всех систем формируется только фаза с ГЦК-решеткой, без явно выраженной текстуры в нитридных слоях. Для ZrN и CrN фазы с ГЦК-решеткой являются равновесными, а для NbN – неравновесными. Увеличение толщины нитридных слоев приводит к появлению текстуры в ZrN/Cu- и CrN/Cu-системах и формированию равновесной ε-NbN-фазы в слоях системы NbN/Cu. Испытания на коррозионную стойкость в среде образования хлорид-ионов показали, что покрытия имеют анодный характер. Наилучшие коррозионные свойства были получены для покрытий с наименьшей толщиной слоев (около 8…10 нм).

СТРУКТУРА І КОРОЗІЙНА СТІЙКІСТЬ ВАКУУМНО-ДУГОВИХ БАГАТОПЕРІОДНИХ CrN/Cu-, ZrN/Cu- ТА NbN/Cu-ПОКРИТТІВ

Г.О. Постельник, О.В. Соболь, В.О. Столбовий, І.В. Сердюк, O. Chocholaty

Проведено дослідження структури і властивостей вакуумно-дугових багатоперіодних композиційних покриттів системи MeN/Cu (де Me – Cr, Zr і Nb). Встановлено, що при найменшій товщині наношарів (близько 8…10 нм) композитів у шарах всіх систем формується тільки фаза з ГЦК-решіткою, без помітно вираженої текстури в нітридних шарах. Для ZrN і CrN фази з ГЦК-решітками є рівноважними, а для NbN – нерівноважними. Збільшення товщини нітридних шарів призводить до появи текстури в ZrN/Cu- та CrN/Cu-системах і формування рівноважної ε-NbN-фази в шарах системи NbN/Cu. Випробування на корозійну стійкість у середовищі утворення хлорид-іонів показали, що покриття мають анодний характер. Найкращі корозійні властивості були отримані для покриттів з найменшою товщиною шарів (близько 8…10 нм).